LIMNOLOGY
and
OCEANOGRAPHY: METHODS

ASLO

Limnol. Oceanogr.: Methods 00, 2016, 00–00

doi: 10.1002/lom3.10095

A cost-effective image processing approach for analyzing the ecohydrology of river corridors

Tyler A. Keys,*[1] C. Nathan Jones,[2] Durelle T. Scott,[1] Daniel Chuquin[1]
[1]Virginia Tech, Department of Biological Systems Engineering, Blacksburg, Virginia
[2]Virginia Tech, Department of Forest Resources and Environmental Conservation, Blacksburg, Virginia

Abstract

There is currently a need for robust, high-resolution monitoring techniques to assess and quantify ecosystem dynamics within surface water bodies and their riparian ecosystems. This study presents a cost effective, user-friendly technique for examining the ecohydrology of stream and river corridors through the use of digital imagery. Using a simple digital camera, we captured hourly images of a small portion of a headwater Appalachian stream and adjacent floodplain. Then, we used pixel classification techniques to evaluate ecohydrologic parameters (e.g., inundation surface area, floodplain wetness, and vegetation dynamics) in each image. Results highlight the episodic nature of river floodplain connectivity, variation in surface wetness across the gradient from river to upland ecosystems, and the seasonal variability of vegetation density and health. To validate the accuracy of image-based measurements, we then compared inundation area estimates to an existing inundation model and found a high level of agreement ($R^2 = 0.94$; NRMSE = 7.96%). Our study highlights the use of time-lapse imagery as a robust, cost-effective method to capture the dynamics of river corridors and associated ecosystem services.

The study of interactions between water resources and their surrounding ecosystems, known as ecohydrology, is a critical component of evaluating and conserving ecosystem services (Rodriguez-Iturbe 2000; Braumen et al. 2007; Grygoruk and Acreman 2015). Of particular interest, riparian and floodplain ecosystems provide many critical ecosystem services, ranging from increased biodiversity (Naiman et al. 1993; Harding et al. 1998), flood peak attenuation (Sheaffer et al. 2002), and biogeochemical processing of reactive solutes (Scott et al. 2014; Boudell et al. 2015). While riparian zones and floodplains have been studied extensively (e.g., Tockner and Stanford 2002), much of our understanding is based on coarse resolution observations in both spatial and temporal domains (Kirchner et al. 2004).

Because of the economic impact and ecological importance of flooding, a great deal of effort has been invested in mapping inundation extent in floodplains. Methods range from hydrodynamic modeling (e.g., Hunter et al. 2007), remote sensing (e.g., Vanderhoof et al. 2015), and even tree ring record analysis (e.g., Ballesteros et al. 2011). While these methods can produce fairly reliable estimates of inundation, they often lack proper validation techniques because of the lack of high resolution data and the episodic nature of flooding. For example, the U. S. Army Corps of Engineers' River Analysis System (HEC-RAS) model is often used to estimate inundation extent. However, because there is a great deal of uncertainty typically associated with the model inputs (e.g., channel bathymetry, stream flow, hydraulic roughness coefficients) and because validation data is typically not available, there is often considerable error associated with the modeled inundation extent (Merwade et al. 2008a). Several remote sensing products such as Light Detection and Ranging (LiDAR) and multispectral imagery have been used to characterize inundation extent and other relevant hydrogeomorphic parameters. Traditionally, LiDAR has been used to measure high resolution topographic data (Cook and Merwade 2009; Bates 2012; Saksena and Merwade 2015). However, other relevant uses of LiDAR include the assessment of geomorphic stability (Resop and Hession 2010), measurement of habitat structure and diversity (Milan et al. 2010; Resop et al. 2012), and quantification of vegetative roughness (Straatsma and Baptist 2008; Abu-Aly et al. 2014). Recent advancements in LiDAR data have also allowed for the detection of inundated areas (Lang and McCarty 2009; Milan and Heritage 2012) and even the measurement of channel bathymetry (Hilldale and Raff 2008; Skinner 2011). Multispectral imagery has also been used in a wide variety of fluvial studies for mapping stream features (e.g., Leckie et al.

Additional Supporting Information may be found in the online version of this article.

*Correspondence: tkeys@vt.edu

2005) and monitoring stream morphology (e.g., Wright et al. 2000). While these methods can delineate stream inundation with high accuracy, data collection remains relatively expensive and time consuming, and thus, there is a need to develop low-cost alternatives.

Identification of "wet areas" across the landscape is also of interest for both our mechanistic understanding of ecosystem processes and from a regulatory perspective. Specifically, saturated soils drive many redox processes that lead to biogeochemical transformations including denitrification (e.g., Anderson et al. 2015), carbon sequestration (e.g., Davidson and Janssens 2006), and greenhouse gas production (e.g., Batson et al. 2015). Because of the spatial and temporal heterogeneity of both surface and subsurface flowpaths in floodplains and riparian zones, redox conditions and associated biogeochemical processes are often intermittent and difficult to measure and generalize (Vidon et al. 2015). Currently, soil moisture is characterized through point measurements and/or remote sensing (Dobriyal et al. 2012). However, point measurements are often misleading because the heterogeneity associated with riparian soils and remote sensing often restricts the ability to capture temporal variations. This often complicates regulatory decisions associated with wetland delineation, where wetland hydrologic conditions must be proven through a series of visual indicators and/or shallow well installations (Fennessy et al. 2004). Therefore, both the research and regulatory communities would benefit from the development of a new, low cost technique that robustly identifies "wet areas" with both high spatial and temporal resolutions.

Seasonal vegetation dynamics are also crucial to understand when investigating riparian ecosystem processes. Vegetation phenology can be used as a measure of ecosystem productivity (Field et al. 1995) as well as an indicator of overall ecosystem health (Baird and Wilby 1999). Moreover, vegetation metrics can be used as auxiliary information to aid in data interpretation from other sensors. At a broad scale, multispectral vegetation indices can be used as a remotely sensed metric to assess both terrestrial and aquatic vegetation dynamics. Most commonly used is the normalized difference vegetation index (NDVI), which calculates the difference between the near infrared and red spectral bands. The NDVI has been widely used in the field of remote sensing as a measure of vegetative greenness and overall ecosystem health (e.g., DeFries and Townshend 1994; Pettorelli et al. 2005). However when raster data are only comprised of three spectral bands, as is the case for Red Green Blue (RGB) digital imagery, multispectral vegetation indices such as the NDVI cannot be used. This becomes problematic when investigating riparian ecosystems as freely available satellite remote sensing does not have the spatial or temporal resolution necessary to accurately analyze riparian ecosystems. Similar to landscape moisture metrics, there is currently a need for high resolution spatiotemporal measurements of riparian and floodplain vegetation dynamics.

Here, we outline an approach to measure ecohydrologic parameters within riparian zones and floodplains through the use of time-lapse imagery. We demonstrate the measurement of three critical parameters within the context of ecohydrology, an emerging field with a dearth of research focusing on monitoring and assessment techniques. While the complex coupling of disciplines within ecohydrology has hindered high resolution ecohydrologic monitoring thus far (Krause et al. 2015), there is a great need for innovative techniques that can overcome the challenges associated with measuring temporally and spatially heterogeneous processes. The methodology described in this article fills such a gap with a straight forward, inexpensive, and robust monitoring system. A comprehensive workflow of our methodology is provided within the following sections to ensure that this methodology can be easily replicated and improved on.

Materials and procedures

Site description

We used the Virginia Tech *Stream Restoration, Education, and Management Lab* (StREAM Lab) to conduct this study. The StREAM Lab is located along Stroubles Creek, a recently restored third order stream in the Ridge and Valley physiographic province in southwestern Virginia, U.S.A. (Fig. 1). Until the restoration in 2009, the riparian area was used for hay production and grazing. Since then, successional riparian vegetation has been established and depressional floodplain wetlands have emerged. The Stroubles Creek watershed has an area of approximately 15 km^2 and is comprised of 84% urban/residential landcover, 13% agriculture, and 3% forest (Jin et al. 2013). Stroubles Creek reaches bankfull conditions ($\sim 2\ m^3/s$) approximately three times per year, resulting in minor inundation of adjacent floodplain wetlands. Further, depressional wetlands experience inundation periodically from the surficial aquifer and upslope water flowpaths. However, evapotranspiration limits soil saturation and inundation of depressional wetlands during the growing season. Stroubles Creek is an ideal location for this study because it contains multiple stream gages and is a third order stream, making it unidentifiable in satellite imagery.

Hourly images of the southern portion of Stroubles Creek (Fig. 1) were obtained from a NetCam XL network camera (Fig. 2a). The camera was placed on top of a field tower at a height of 10 m and positioned with an angle of 30° from the horizontal (Fig. 2b). To minimize light reflection from the sun, the camera was pointed southerly. The camera and a Campbell CR1000 datalogger were powered using a deep cycle marine battery (group size 27) augmented with solar power from a BP 65-Watt solar panel. Images were taken every hour on the hour, stored on the datalogger, and transmitted to a server via a spread spectrum radio network. Real

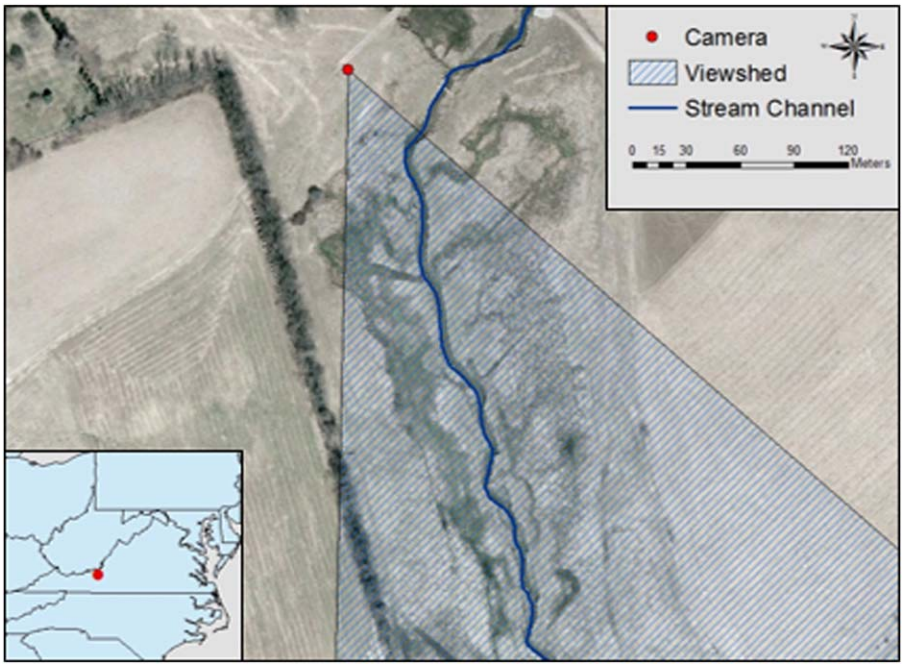

Fig. 1. Site map illustrating the location of the camera, its viewshed, and the stream channel.

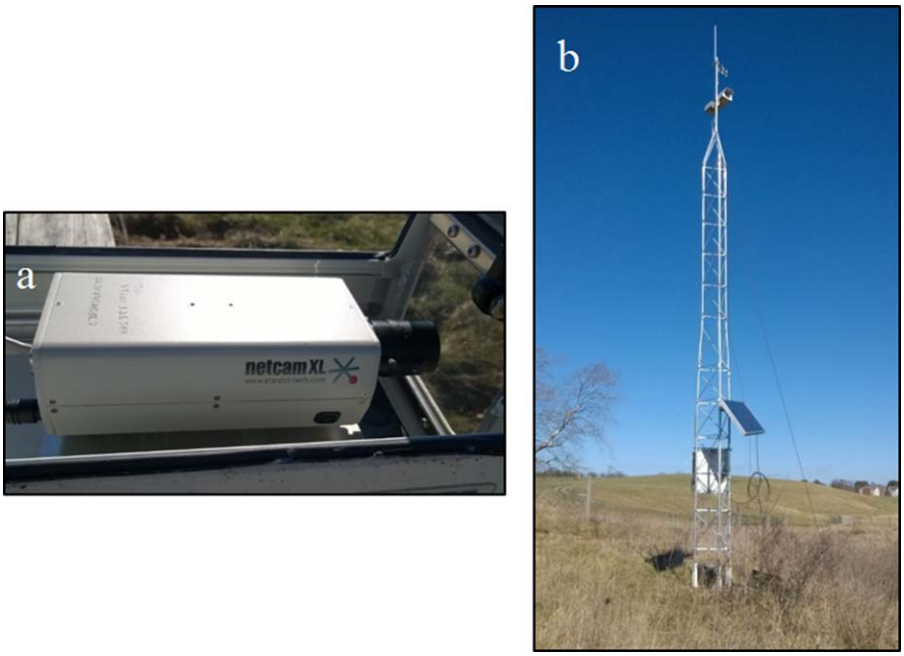

Fig. 2. (**a**) Close up view of the NetCam XL network digital camera, (**b**) site setup illustrating the tower and camera setup.

time imagery, stream flow, and meteorological parameters can be seen in real time at streamlab.bse.vt.edu.

Image processing

Once compiled within the database, digital images were processed by a MATLAB script which can be found in the supplementary material. Similar to Royem et al. (2012), which used digital image processing to determine stream stage at a single location, our MATLAB script was developed to incorporate a variety of spatial metrics including flow characteristics, floodplain saturation, and vegetation dynamics. The MATLAB routine consists of three primary

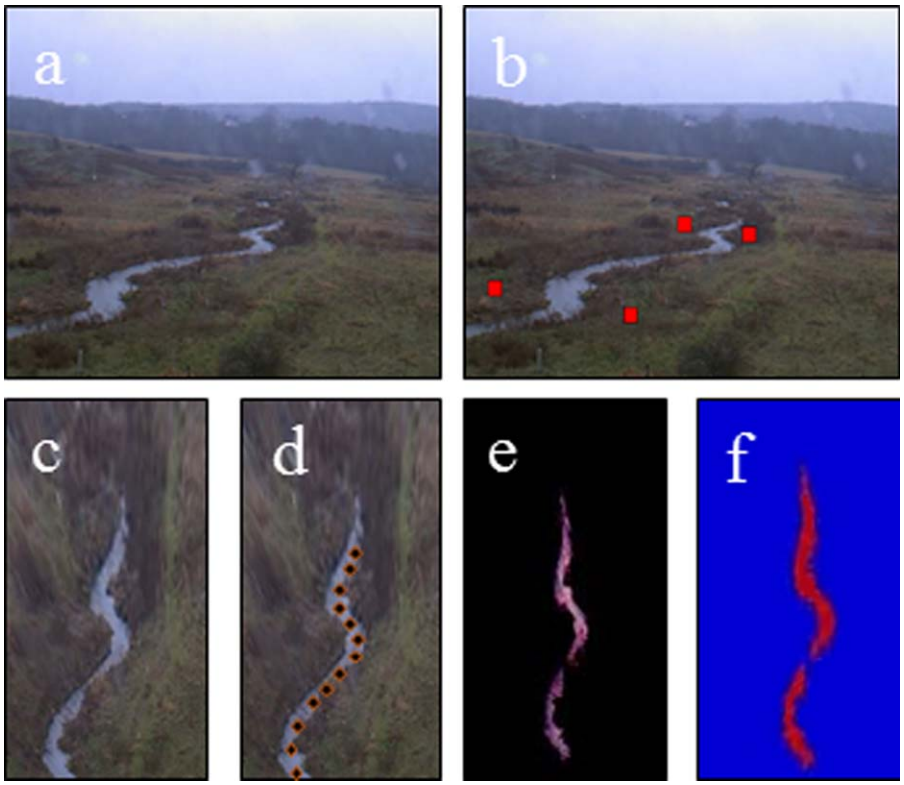

Fig. 3. (**a**) Plain image selected by user, (**b**) image with identified ground control points, (**c**) orthorectified ROI, (**d**) classification points within ROI, (**e**) enhanced image mask and (f) final processed image with binary mask.

steps: (1) image rectification, (2) region of interest (ROI) selection, and (3) image analysis. In the first step, image rectification converts the pixels within an image to correspond to the ground footprint. Four known ground control points (GCPs) are identified by the user within the image to adjust to the selected scale. The GCPs correspond to surveyed points on the ground that form a rectangle. Input distances based on this known geometry are required to adjust the image such that the rest of the image is converted to the same scale. Knowing and defining the exact location of GCPs is the most critical component of the analysis. If GPCs are not correctly identified, the image will not be correctly adjusted, resulting in inaccurate quantitative measurements. After GCP selection, the image is orthorectified to remove image distortion caused by the oblique camera angle. During step 2, a graphical user interface is used to select the appropriate ROI within the orthorectified image. In step 3, image classification is performed to delineate wet vs. dry pixels. The user identifies wet pixels within the image and water bodies are identified by the MATLAB script based on the user's selection of wet pixels.

Image wetness analysis

The purpose of selecting classification points is to identify pixels within the ROI that can reasonably be considered "wet" areas. Based on the user identified points, a supervised classification is performed so that all pixels within the image that have reflectance values similar to the selected pixels will be classified into different spectral classes. The entire image is then converted to a binary matrix, where each pixel in the image is assigned a value of zero (dry) or one (wet). Pixels classified as wet are automatically summed up and displayed in the output text file. To convert the pixel area to actual area, the output pixel area must multiplied by the spatial resolution of each image. Spatial resolution can be determined by measuring the actual area of the ROI and dividing by the number of pixels corresponding to that area. An illustration of the entire water segmentation process can be seen in Fig. 3.

To further analyze flooding dynamics, our code locates wet areas on the floodplain as well as their degree of wetness. After the binary mask has separated wet pixels from dry pixels, degree of wetness is determined by creating a pixel-based color map. All wet pixels on the image are assigned a value based on their similarity to the user's selected classification pixels, where wet pixels are assigned a greater value than dry pixels. For example, the stream is given the highest value as it has the closest values to the classification points in every image. Values for large floodplain "hotspots" are assigned values that are less than the

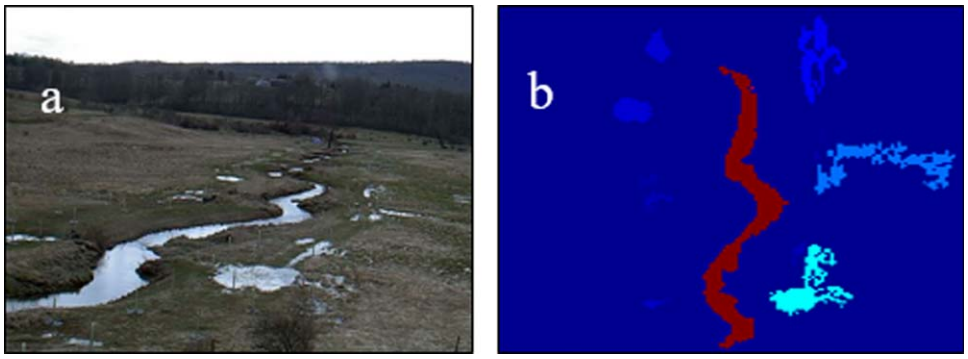

Fig. 4. (**a**) Image of Stroubles Creek and areas of wetness on the floodplain, (**b**) classified image showing the degree of inundation across the image. The gradient in pixel color represents the degree of similarity between the given pixels and the user selected classification pixels, where dark red signifies a high degree of similarity and dark blue signifies no similarity.

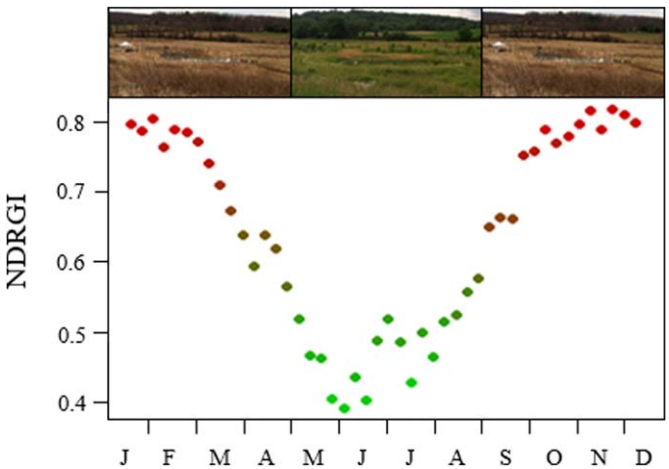

Fig. 5. Values of NDRGI for weekly images over the course of the 2012 calendar year. Representative images of floodplain vegetation are shown above the corresponding growing seasons.

main channel but are still greater than dry pixels. This clearly separates the stream channel from dry land while still being able to identify floodplain hotspots. As illustrated in Fig. 4, the stream channel and wet areas on the floodplain are not only identified, but also separated based on their degree of wetness.

Vegetation analysis

The final metric measured by our algorithm is floodplain vegetation dynamics. To overcome the challenge of analyzing vegetation dynamics without multispectral vegetation indices, the Normalized Difference Red Green Index (NDRGI) as calculated below (Eq. 1) was applied to all images.

$$\mathrm{NDRGI} = \frac{\rho_{\mathrm{Red}} - \rho_{\mathrm{Green}}}{\rho_{\mathrm{Red}} + \rho_{\mathrm{Green}}} \quad (1)$$

The NDRGI measures vegetative greenness based on difference between the reflectance values of the red (ρ_{Red}) and green (ρ_{Green}) spectral bands on a scale from 0 to 1 with a value of 0 corresponding to entirely green vegetation and a value of 1 corresponding to completely dormant vegetation (Yang et al. 2008; Stott et al. 2015). The index is highly transferable as it can be derived from any camera which produces images in RGB color space. This includes almost all forms of digital imagery, including satellite imagery. However, adjusting a camera's color space settings could constrain or inhibit the calculation of the index. Unlike wetness indices, calculation of NDRGI only depends on step 1 and step 2 in the MATLAB script: image rectification and ROI selection. Image classification has no impact on the calculated value of NDRGI because the calculations are based on stored reflectance values from the pixels in the image. For this study, weekly NDRGI values for an entire calendar year were plotted to examine the seasonal variation in floodplain vegetation dynamics (Fig. 5). The plot shows that NDRGI values are highest during the winter months when vegetation is dormant and lowest during summer months when vegetation is photosynthetically active. Corresponding images of the floodplain during the different seasons are displayed as a form of visual verification.

Assessment

Proof-of-concept

To validate the ability of our code to evaluate inundated surface area, we compared inundation area measured in camera imagery with inundation estimates from a previously developed inundation model. Described in Jones et al. (2015), the inundation model utilizes a digital terrain model of the floodplain and stage data measured at the site. The terrain model was derived from a combination of high resolution LiDAR and measured channel bathymetry, and developed using methods outlined by Merwade et al. (2008b). LiDAR data was provided by the City of Blacksburg. Data was collected in November of 2011, groundtruthed with a root mean square error of 1 m horizontally and 18 cm

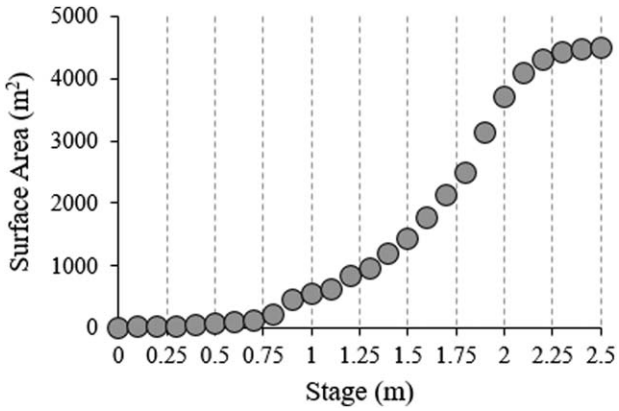

Fig. 6. Relationship between stream stage and surface area resulting from the inundation model. Circles represent the modeled surface area at incremental stream stage values.

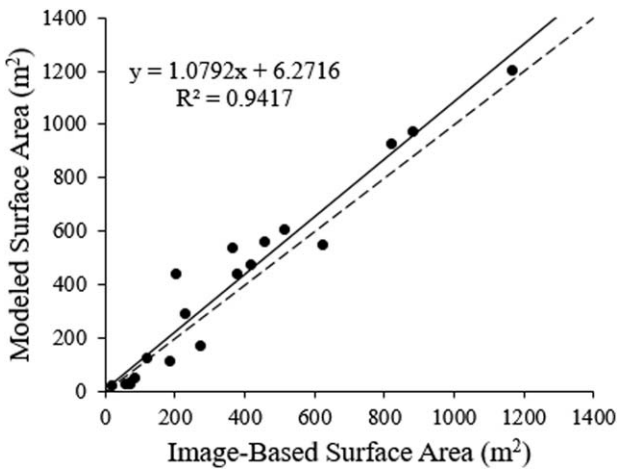

Fig. 7. Comparison between modeled surface area and image-based estimations of surface area for 20 independent storm events. The dotted line represents the 1 : 1 ratio while the solid line represents the linear least squares regression line.

vertically, and point spacing of 1.4 m. Channel bathymetry data was measured using a real-time kinematic geographic positioning system (RTK-GPS, Topcon GR-3). The resulting digital elevation model has a 1 m by 1 m grid. Then, inundation was estimated using conditional raster analysis similar to the method presented in Jones et al. (2008). The stage-surface area relationship from the model is shown in Fig. 6.

For validation, individual images from 20 independent 2012 storm events were selected and analyzed. Image based surface area estimations were matched with stream stage values measured at the same exact time via a pressure transducer in the thalweg of the stream. Corresponding modeled surface area estimates were determined based on the stage-surface area relationship. Results between methods were then compared using a simple regression analysis. The coefficient of determination (R^2), slope, and normalized root-mean-square error (Eq. 2) were then calculated to determine goodness of fit of the data.

$$\mathrm{NRMSE} = \frac{\sqrt{\frac{\sum_{i=1}^{n}(\hat{y}-y)}{n}}}{y_{max}-y_{min}} \tag{2}$$

The NRMSE as shown above is a measure of residual variance, where $\hat{y}$ is the image based surface area estimations, y is modeled surface area estimations, and y_{max}–y_{min} is the range of the modeled surface area values. The regression analysis between estimates from the two methodologies (Fig. 7) resulted in a fairly linear relationship with a regression coefficient of determination (R^2) value of 0.9417, a slope of 1.0792, and a normalized root-mean-square error (NRMSE) of 7.96%, suggesting a strong correlation between the results. It should be noted that while there is a strong correlation between the modeled and image based estimations, modeled surface area predictions produced slightly higher values than image based estimations. This can be seen in Fig. 6 where the regression line is slightly greater than the 1: 1 ratio line, with a slope of 1.0792. These results are likely due to the visual obstruction of water created by the riparian vegetation and stream banks.

Limitations

While this new methodology can be easily implemented in a variety of environments, it should be noted that several limitations on applicability exist. First, stream visibility is limited during periods of low flow and high vegetation. The result of this error can be seen in the larger amount of variation associated with estimated inundation surface areas during periods of low flow in comparison with the relatively accurate estimations during periods of high flow. In the field of ecohydrology, high flows can be of greater interest than low flows as higher flows signify periods of time in which stream channels are hydrologically connected with their adjacent floodplains.

Second, water droplets on the camera lens can greatly distort or obstruct the camera's view during rain events or early in the morning due to the accumulation of dew. During storm events, water droplets can descend down the camera lens, distorting the image if on the lens at the instant when the image is taken. While this was generally not an issue in the majority of our images, instances of heavy precipitation did result in image distortion. During winter months, water on the camera can freeze, resulting in ice on the camera lens. This phenomenon generally occurs early in the morning when frost from the night before has accumulated on the surface of the camera lens. However by midday, none of the images were affected by ice on the camera lens.

Third, our system can only analyze images acquired during the day due to the limited spectral range of the imagery. The absence of nighttime data does not affect the ability to

analyze vegetation dynamics, which do not change overnight but rather throughout seasons. However, flood events can occur entirely during the course of a single night due to the stochastic nature of flooding. Without nighttime data, it can be challenging to fully understand the ecohydrology of a system without other continuous variables (e.g., stream stage). Data could be retrieved in the dark using a thermal or infrared camera. For example, infrared cameras have been used for analyzing hillslope and riparian saturation dynamics (Pfister et al. 2010) as well as wildlife habits (Claridge et al. 2005).

The fourth and final notable limitation with our code is that it relies on user selection of GCPs, ROIs, and classification points. As mentioned above, precise identification of GCPs is the most crucial aspect of the analysis. Error associated with ROI selection should be relatively low as this step is simply the selection of the analysis area in question. Classification point selection plays an important role in water identification and quantification. While this does not affect vegetation characteristic estimations which are calculated solely based on RGB reflectance values, water separability is greatly influenced by the selection of classification points. Thus the degree of accuracy in water based calculations has the potential for both random and systematic error based on the user. For example, user error could be the result of accidentally picking a dry area as a classification point or selecting a dry area that appears to be a wet. Despite its limitations and potential for error, the methodology provides a relatively simple and accurate process for monitoring surface water bodies.

Discussion

A great deal of research has been conducted on ecohydrologic dynamics of large surface water bodies and global ecohydrology (Jackson et al. 2009); nonetheless, very little research has focused on the ecohydrology of local water bodies (Janauer 2000), which play a vital role in the overall context of ecohydrology. Furthermore, previous studies have expressed the importance of analyzing ecohydrology across scales with particular emphasis on the combination of large scale remote sensing and modeling with small scale monitoring (Janauer 2000; Asbjornsen et al. 2011). The methodology described in this article presents a useful new approach for monitoring and analysis of ecohydrology at multiple scales. Additionally, the presented applications illustrate just several of the many potential usages of our new methodology.

Digital imagery can be used for analyzing a variety of environmental parameters and water bodies while allowing for spatial monitoring and scaling of these variables. One such example is forested water bodies such as streams and wetlands. Forested streams and wetlands are extremely important ecosystems which provide services such as water quality improvement, flood control, and wildlife habitat (Walbridge 1993). However, monitoring of forested systems is a major challenge as canopy cover limits the ability of freely available remote sensing to identify forested water bodies (Ozesmi and Bauer 2002) and placing monitoring equipment in remote areas can be problematic. Innovative monitoring techniques such as our image processing approach allow for spatial and temporal studies in isolated regions without logistical issues such as transporting expensive instruments to remote locations and the dangers of consistent fieldwork in unsafe areas.

Urban streams would also benefit from this low cost monitoring system as urban systems are constantly changing and often unmonitored (Hughes and Yeakley 2014). Moreover, urban stream management is generally focused on flood prevention as opposed to maintaining natural flow regimes (Zalewski and Wagner 2005). The sharp contrast between low flows and sudden high flows generated from urban storm runoff can have considerable effects on stream channel-floodplain interactions and overall ecosystem health. Challenges in urban systems such as water quality degradation, habitat fragmentation, and bank erosion are difficult to address due to a lack of monitoring and public involvement (Hughes et al. 2014). Adding to these issues, storm events are often unsafe to monitor firsthand and do not get thoroughly analyzed as a result. Furthermore, large floods can be difficult to monitor when fixed gauging stations are destroyed by high flows. These issues will be intensified by rapid urbanization and increased flooding, and thus, there is a great need for innovative monitoring techniques to overcome these obstacles. Imagery can provide valuable information (e.g., flood extent and discharge) during extreme events without being destroyed by the events themselves. Digital imagery approaches such as ours provide a new manner of addressing these challenges presented by urbanization.

The field of stream restoration has rapidly developed over the previous 20 yr (Palmer et al. 2014) with a myriad of projects being undertaken across the U.S. (Bernhardt et al. 2005) and in Europe (Ormerod 2004). However, a lack of monitoring frameworks and post project monitoring funding has limited the ability to address the successfulness of restoration projects (Buchanan et al. 2014; Morandi et al. 2014). Our methodology presents a new approach for monitoring stream restoration for long periods of time following project completion. Through digital imagery, one could observe a variety of parameters such as changes in stream channel geomorphology, successional vegetation, and success of planted trees. This idea diverges from the belief that large amounts of money and resources are necessary to monitor long term effects of stream restoration.

Crowdsourcing

The developed MATLAB code is robust enough that minimal alterations of the code allow for it to be implemented in a wide variety of environments. Furthermore, the code can

be easily transferred to other programming languages or converted into an executable, so that users do not need a MATLAB license to use the script. Our code was developed this way because one of the key concepts of this study is to advance the idea of crowdsourcing and citizen science. Crowdsourcing can be defined as the participation of the general public in compiling data via the internet to be used for the greater good of society (Estellés-Arolas and González-Ladrón-de-Guevara 2012). Citizen science has become prominent in environmental fields such as hydrology and ecology as environmental protection requires active participation from the general public (Buytaert et al. 2014). Despite its simplicity and voluntary nature, crowdsourcing has been a highly effective source of innovation in various environmental disciplines (Brabham 2013). The monitoring methodology described in this article lends itself well to innovative forms of crowdsourcing in multiple environmental fields. While our study utilizes a field camera, contemporary cellular phone cameras can be almost equally as effective in acquiring relatively high resolution digital images. With the advancement of smartphones, geographically referenced or geotagged images can be obtained via a smartphone camera and sent to a database. This allows for a crowdsourced monitoring approach which can be implemented in practically any location across the globe.

Comments and recommendations

The following guidelines are provided as a basis for future studies or deployment. If performing a time-lapse analysis such as the one in our study, it is essential that the camera to be used can withstand environmental conditions such as precipitation and extreme temperatures. Depending on the length and scope of the project, a variety of camera options can be used. While our study used a high-tech camera, field cameras such as a trail and game cameras are readily available and relatively inexpensive ($\sim$ \$100). Similar to camera selection, camera placement should aid in optimizing the image analysis for specific questions. For example, placing the camera near the stream at a low elevation will provide coverage across all flow regimes, whereas higher placement (e.g., a tower) will provide greater spatial coverage. If at all possible, the camera should be directed due North or due South to avoid light interference from the sun's East to West movement. Positioning the camera in an area which is exposed to sunlight is necessary in colder regions where ice could accumulate on the camera lens. On the contrary, the camera should be placed in a shaded area if the local climate is warm and excess sun could potentially overheat the camera.

To use the methodology as a form of crowdsourcing, a variety of image acquisition approaches can be used. For example, images from cell phones could be taken from a specified location or within a given region and sent to a database. Alternatively, designated areas could be set up so that images are taken at a precise monitoring location. This would be ideal in areas with large numbers of tourists visiting. For example, supraglacial streams in subarctic regions such as Alaska receive a great number of annual tourists and are also at the center of ecohydrology research due to drastically changing hydrology and nutrient fluxes (Hood and Scott 2008; Blaen et al. 2014). Another example of potential applicability exists in developing countries where cameras are in abundance yet environmental data is scarce. For example, Frommberger and Schmid (2013) implemented a disaster reporting system based on crowdsourcing from smartphones in Laos, a developing nation with very little publicly available environmental information. As the world continues to develop and environmental issues become greater, the incorporation of crowdsourcing into the field of ecohydrology will become increasingly more important.

The future of research in ecohydrology depends largely on a paradigm shift from the complex, discipline specific approach taken in research to a simplified yet holistic ecosystem approach. Thus far, an interdisciplinary manner has only been applied at a broad scale while neglecting local scale ecohydrology. The methodology described in this article presents a breakthrough that bridges the gap between scales in the field of ecohydrology. While not without limitations, our new method provides a low-cost, user friendly, and widely applicable ecohydrologic monitoring system. Ideally, future studies will be able to improve on the methodology by reducing its limitations and using it as a means of crowdsourcing.

References

Abu-Aly, T. R., G. B. Pasternack, J. R. Wyrick, R. Barker, D. Massa, and T. Johnson. 2014. Effects of LiDAR-derived, spatially distributed vegetation roughness on two-dimensional hydraulics in a gravel-cobble river at flows of 0.2 to 20 times bankfull. Geomorphology **206**: 468–482. doi:10.1016/j.geomorph.2013.10.017

Anderson, T. R., P. M. Groffman, and M. T. Walter. 2015. Using a soil topographic index to distribute denitrification fluxes across a northeastern headwater catchment. J. Hydrol. **522**: 123–134. doi:10.1016/j.jhydrol.2014.12.043

Asbjornsen, H., and others. 2011. Ecohydrological advances and applications in plant–water relations research: A review. J. Plant Ecol. **4**: 3–22. doi:10.1093/jpe/rtr005

Baird, A. J., and R. L. Wilby. 1999. Eco-hydrology: Plants and water in terrestrial and aquatic environments. Routledge Press.

Ballesteros, J. A., J. M. Bodoque, A. Díez-Herrero, M. Sanchez-Silva, and M. Stoffel. 2011. Calibration of floodplain roughness and estimation of flood discharge based on tree-ring evidence and hydraulic modelling. J. Hydrol. **403**: 103–115. doi:10.1016/j.jhydrol.2011.03.045

Bates, P. D. 2012. Integrating remote sensing data with flood inundation models: How far have we got? Hydrol. Process. **26**: 2515–2521. doi:10.1002/hyp.9374

Batson, J., G. B. Noe, C. R. Hupp, K. W. Krauss, N. B. Rybicki, and E. R. Schenk. 2015. Soil greenhouse gas emissions and carbon budgeting in a short-hydroperiod floodplain wetland. J. Geophys. Res. Biogeosci. **120**: 77–95. doi:10.1002/2014JG002817

Bernhardt, E. S., and others. 2005. Synthesizing U. S. river restoration efforts. Science **308**: 636–637. doi:10.1126/science.1109769

Blaen, P. J., A. M. Milner, D. M. Hannah, J. E. Brittain, and L. E. Brown. 2014. Impact of changing hydrology on nutrient uptake in high arctic rivers. River Res. Appl. **30**: 1073–1083. doi:10.1002/rra.2706

Boudell, J. A., M. D. Dixon, S. B. Rood, and J. C. Stromberg. 2015. Restoring functional riparian ecosystems: Concepts and applications. Ecohydrology **8**: 747–752. doi:10.1002/eco.1664

Brabham, D. C. 2013. Crowdsourcing. MIT Press.

Brauman, K. A., G. C. Daily, T. K. E. Duarte, and H. A. Mooney. 2007. The nature and value of ecosystem services: an overview highlighting hydrologic services. Annu. Rev. Env. Resour. **32**: 67–98. doi:10.1146/annurev.energy.32.031306.102758

Buchanan, B. P., G. N. Nagle, and M. T. Walter. 2014. Long-term monitoring and assessment of a stream restoration project in central New York. River Res. Appl. **30**: 245–258. doi:10.1002/rra.2639

Buytaert, W., and others. 2014. Citizen science in hydrology and water resources: Opportunities for knowledge generation, ecosystem service management, and sustainable development. Front. Earth Sci. **2**: 1–21. doi:10.3389/feart.2014.00026

Claridge, A. W., G. Mifsud, J. Dawson, and M. J. Saxon. 2005. Use of infrared digital cameras to investigate aspects of the social behaviour of cryptic species. Wildlife Res. **31**: 645–650. doi:10.1071/WR03072

Cook, A., and V. Merwade. 2009. Effect of topographic data, geometric configuration and modeling approach on flood inundation mapping. J. Hydrol. **377**: 131–142. doi:10.1016/j.jhydrol.2009.08.015

Davidson, E. A., and I. A. Janssen. 2006. Temperature sensitivity of soil carbon decomposition and feedbacks to climate change. Nature. **440**: 165–173. doi:10.1038/nature04514

DeFries, R. S., and J. R. G. Townshend. 1994. NDVI-derived land cover classifications at a global scale. Int. J. Remote Sens. **15**: 3567–3586. doi:10.1080/01431169408954345

Dobriyal, P., A. Qureshi, R. Badola, and S. A. Hussain. 2012. A review of the methods available for estimating soil moisture and its implications for water resource management. J. Hydrol. **458**: 110–117. doi:10.1016/j.jhydrol.2012.06.021

Estellés-Arolas, E., and F. González-Ladrón-de-Guevara. 2012. Towards an integrated crowdsourcing definition. J. Inf. Sci. **38**: 189–200. doi:10.1177/0165551512437638

Fennessy, M. S., A. D. Jacobs, and M. E. Kentula. 2004. Review of rapid methods for assessing wetland condition. EPA/620/R-04/009. US Environmental Protection Agency, Washington, DC.

Field, C. B., J. T. Randerson, and C. M. Malmström. 1995. Global net primary production: Combining ecology and remote sensing. Remote Sens. Environ. **51**: 74–88. doi:10.1016/0034-4257(94)00066-V

Frommberger, L., and F. Schmid. 2013. Crowdsourced bidirectional disaster reporting and alerting on smartphones in Lao PDR. arXiv preprint arXiv:1312.6036.

Grygoruk, M., and M. Acreman. 2015. Restoration and management of riparian and riverine ecosystems: Ecohydrological experiences, tools and perspectives. Ecohydrol. Hydrobiol. **15**: 109–110. doi:10.1016/j.ecohyd.2015.07.002

Harding, J. S., E. F. Benfield, P. V. Bolstad, G. S. Helfman, and E. B. D. Jones. 1998. Stream biodiversity: The ghost of land use past. Proc. Natl. Acad. Sci. U.S.A. **95**: 14843–14847, doi:10.1073/pnas.95.25.14843

Hilldale, R. C., and D. Raff. 2008. Assessing the ability of airborne LiDAR to map river bathymetry. Earth Surf. Proc. Land. **33**: 773–783. doi:10.1002/esp.1575

Hood, E., and D. Scott. 2008. Riverine organic matter and nutrients in southeast Alaska affected by glacial coverage. Nat. Geosci. **1**: 583–587. doi:10.1038/ngeo280

Hughes, R. M., and J. A. Yeakley. 2014. Major research and monitoring needs for urban streams and watersheds, p. 243–252. *In* J. A. Yeakley, K. G. Maas-Hebner, and R. M. Hughes [eds.], Wild salmonids in the urbanizing pacific northwest. Springer.

Hughes, R. M., and others. 2014. A review of urban water body challenges and approaches: (1) Rehabilitation and remediation. Fisheries **39**: 18–29. doi:10.1080/03632415.2013.836500

Hunter, N. M., P. D. Bates, M. S. Horritt, M. D. Wilson. 2007. Simple spatially-distributed models for predicting flood inundation: a review. Geomorphology **90**: 208–225. doi:10.1016/j.geomorph.2006.10.021

Jackson, R. B., E. G. Jobbágy, and M. D. Nosetto. 2009. Ecohydrology in a human-dominated landscape. Ecohydrology **2**: 383–389. doi:10.1002/eco.81

Janauer, G. A. 2000. Ecohydrology: Fusing concepts and scales. Ecol. Eng. **16**: 9–16. doi:10.1016/S0925-8574(00)00072-0

Jin, S., L. Yang, P. Danielson, C. Homer, J. Fry, and G. Xian. 2013. A comprehensive change detection method for updating the National Land Cover Database to circa 2011. Remote Sens. Environ. **132**: 159–175. doi:10.1016/j.rse.2013.01.012

Jones, K., G. Poole, S. O'Daniel, L. Mertes, and J. Stanford. 2008. Surface hydrology of low-relief landscapes: Assessing surface water flow impedance using LIDAR-derived digital elevation models. Remote Sens. Environ. **112**: 4148–4158. doi:10.1016/j.rse.2008.01.024

Jones, C. N., D. T. Scott, C. R. Guth, E. R. Hester, and W. C. Hession. 2015. Seasonal variation in floodplain biogeochemical processing in a restored headwater stream. Environ. Sci. Technol. **49**: 13190–13198. doi:10.1021/acs.est.5b02426

Kirchner, J. W., X. Feng, C. Neal, and A. J. Robson. 2004. The fine structure of water-quality dynamics: The (high-frequency) wave of the future. Hydrol. Process. **18**: 1353–1359. doi:10.1002/hyp.5537

Krause, S., J. Lewandowski, C. N. Dahm, and K. Tockner. 2015. Frontiers in real-time ecohydrology–a paradigm shift in understanding complex environmental systems. Ecohydrology **8**: 529–537. doi:10.1002/eco.1646

Lang, M. W., and G. W. McCarty. 2009. LiDAR intensity for improved detection of inundation below the forest canopy. Wetlands. **29**: 1166–1178. doi:10.1672/08-197.1

Leckie, D. G., E. Cloney, C. Jay, and D. Paradine. 2005. Automated mapping of stream features with high-resolution multispectral imagery. Photogramm. Eng. Remote Sens. **71**: 145–155. doi:10.14358/PERS.71.2.145

Merwade, V., F. Olivera, M. Arabi, and S. Edleman. 2008a. Uncertainty in flood inundation mapping: Current issues and future directions. J. Hydrol. Eng. **13**: 608–620. doi:10.1061/(ASCE)1084-0699(2008)13:7(608)

Merwade, V., A. Cook, and J. Coonrod. 2008b. GIS techniques for creating river terrain models for hydrodynamic modeling and flood inundation mapping. Environ. Model. Softw. **23**: 1300–1311. doi:10.1016/j.envsoft.2008.03.005

Milan, D. J., G. L. Heritage, A. R. G. Large, and N. S. Entwistle. 2010. Mapping hydraulic biotopes using terrestrial laser scan data of water surface properties. Earth Surf. Proc. Land. **35**: 918–931. doi:10.1002/esp.1948

Milan, D. J., and G. L. Heritage. 2012. LiDAR and ADCP use in gravel-bed rivers: Advances since GBR6, p. 286–302. *In* M. Church, P. M. Biron, and A. G. Roy [eds.], Gravel-bed rivers: Processes, tools, environments. Wiley. doi:10.1002/97811199claridg52497.ch22

Morandi, B., H. Piégay, N. Lamouroux, and L. Vaudor. 2014. How is success or failure in river restoration projects evaluated? Feedback from French restoration projects. J. Environ. Manage. **137**: 178–188. doi:10.1016/j.jenvman.2014.02.010

Naiman, R. J., H. Decamps, and M. Pollock. 1993. The role of riparian corridors in maintaining regional biodiversity. Ecol. Appl. **3**: 209–212. doi:10.2307/1941822

Ormerod, S. J. 2004. A golden age of river restoration science? Aquat. Conserv. Mar. Freshw. Ecosyst. **14**: 543–549. doi:10.1002/aqc.663

Ozesmi, S. L., and M. E. Bauer. 2002. Satellite remote sensing of wetlands. Wetl. Ecol. Manage. **10**: 381–402. doi:10.1023/A:1020908432489

Palmer, M. A., K. L. Hondula, and B. J. Koch. 2014. Ecological restoration of streams and rivers: Shifting strategies and shifting goals. Annu. Rev. Ecol. Evol. Syst. **45**: 247–269. doi:10.1146/annurev-ecolsys-120213-091935

Pettorelli, N., J. O. Vik, A. Mysterud, J. M. Gaillard, C. J. Tucker, and N. C. Stenseth. 2005. Using the satellite-derived NDVI to assess ecological responses to environmental change. Trends Ecol. Evol. **20**: 503–510. doi:10.1016/j.tree.2005.05.011

Pfister, L., J. J. McDonnell, C. Hissler, and L. Hoffmann. 2010. Ground-based thermal imagery as a simple, practical tool for mapping saturated area connectivity and dynamics. Hydrol. Process. **24**: 3123–3132. doi:10.1002/hyp.7840

Resop, J. P., and W. C. Hession. 2010. Terrestrial laser scanning for monitoring streambank retreat: Comparison with traditional surveying techniques. J. Hydraul. Eng. **136**: 794–798. doi:10.1061/(ASCE)HY.1943-7900.0000233

Resop, J. P., J. L. Kozarek, and W. C. Hession. 2012. Terrestrial laser scanning for delineating in-stream boulders and quantifying habitat complexity measures. Photogramm. Eng. Remote Sens. **78**: 363–371. doi:10.14358/PERS.78.4.363

Rodriguez-Iturbe, I. 2000. Ecohydrology: A hydrologic perspective of climate-soil-vegetation dynamics. Water Resour. Res. **36**: 3–9. doi:10.1029/1999WR900210

Royem, A. A., C. K. Mui, D. R. Fuka, and M. T. Walter. 2012. Technical note: Proposing a low-tech, affordable, accurate stream stage monitoring system. Trans. ASABE **55**: 237–242. doi:10.13031/2013.42512

Saksena, S., and V. Merwade. 2015. Incorporating the effect of DEM resolution and accuracy for improved flood inundation mapping. J. Hydrol. **530**: 180–194. doi:10.1016/j.jhydrol.2015.09.069

Scott, D. T., R. F. Keim, B. L. Edwards, C. N. Jones, and D. E. Kroes. 2014. Floodplain biogeochemical processing of floodwaters in the Atchafalaya River Basin during the Mississippi River flood of 2011. J. Geophys. Res. Biogeo. **119**: 537–546. doi:10.1002/2013JG002477

Sheaffer, J. R., J. D. Mullan, and N. B. Hinch. 2002. Encouraging wise use of floodplains with market-based incentives. Environ. Sci. Pol. Sustain. Devel. **44**: 32–43. doi:10.1080/00139150209605590

Skinner, K. D. 2011. Evaluation of LiDAR-acquired bathymetric and topographic data accuracy in various hydrogeomorphic settings in the Deadwood and South Fork Boise Rivers, West-Central Idaho, 2007: U.S. Geological Survey Scientific Investigations Report 2011–5051, 30 p.

Stott, D., D. S. Boyd, A. Beck, and A. G. Cohn. 2015. Airborne LiDAR for the detection of archaeological vegetation marks using biomass as a proxy. Remote Sens. **7**: 1594–1618. doi:10.3390/rs70201594

Straatsma, M. W., and M. J. Baptist. 2008. Floodplain roughness parameterization using airborne laser scanning and spectral remote sensing. Remote Sens. Environ. **112**: 1062–1080. doi:10.1016/j.rse.2007.07.012

Tockner, K., and J. A. Stanford. 2002. Riverine flood plains: Present state and future trends. Environ. Conserv. **29**: 308–330. doi:10.1017/S037689290200022X

Vanderhoof, M. K., L. C. Alexander, and M. J. Todd. 2015. Temporal and spatial patterns of wetland extent influence variability of surface water connectivity in the Prairie Pothole Region, United States. Landsc. Ecol. **30**: 1–20. doi:10.1007/s10980-015-0290-5

Vidon, P., S. Marchese, M. Welsh, and S. McMillan. 2015. Short-term spatial and temporal variability in greenhouse gas fluxes in riparian zones. Environ. Monit. Assess. **187**: 1–9. doi:10.1007/s10661-015-4717-x

Walbridge, M. R. 1993. Functions and values of forested wetlands in the southern United States. J. For. **91**: 15–19.

Wright, A., W. A. Marcus, and R. Aspinall. 2000. Evaluation of multispectral, fine scale digital imagery as a tool for mapping stream morphology. Geomorphology **33**: 107–120. doi:10.1016/S0169-555X(99)00117-8

Yang, Z., P. Willis, and R. Mueller. 2008. Impact of band-ratio enhanced AWIFS image to crop classification accuracy. *In* Proceedings of Pecora 17, The Future of Land Imaging Going Operational. November 18–20, 2008, Denver, Colorado, USA.

Zalewski, M., and I. Wagner. 2005. Ecohydrology-the use of water and ecosystem processes for healthy urban environments. Ecohydrol. Hydrobiol. **5**: 263–268.

Acknowledgments

The authors would like to thank Dan Lluch for his help in developing and revising our MATLAB code. We would also like to thank the Virginia Water Resources Research Center for their support with data collection.

Submitted 5 November 2015
Revised 21 January 2016
Accepted 27 January 2016

Associate editor: Paul Kemp